A novel cardiomyocyte enriched microRNA, miR-378, targets IGF1R: implications in post natal cardiac remodeling and cell survival*

Ivana Knezevic[1], Aalok Patel[1], Nagalingam R. Sundaresan[2], Mahesh P. Gupta[2], R. John Solaro[1], Raghu S. Nagalingam[1] and Madhu Gupta[1]

[1]From the Department of Physiology and Biophysics, and Center for Cardiovascular Research, University of Illinois at Chicago, Chicago IL 60612

[2]Department of Surgery, Committee on Cellular and Molecular Physiology, University of Chicago, Chicago, IL 60637

*Running title: *MicroRNA – 378 targets IGF1R and regulates cardiac cell survival*

To whom correspondence should be addressed: Madhu Gupta, Department of Physiology and Biophysics (MC 901), University of Illinois, 835 S. Wolcott Avenue, Chicago, IL, USA, Tel.: (312) 355-4937; Fax: (312) 969-1414; E-mail: guptam@uic.edu

Keywords: microRNA-378; IGF1R, post-natal cardiac remodeling, cardiac apoptosis

---

Background: IGF1/IGF1R signaling promotes cardiomyocyte survival and undergoes down regulation after birth.
Results: Cardiac expression of miR-378 is induced after birth. IGF1R is a direct target of miR-378.
Conclusion: miR-378 promotes cardiac apoptosis.
Significance: Inhibition of miR-378 would be beneficial in promoting cardiac cell survival in an ailing heart.

SUMMARY

Post-natal cardiac remodeling is characterized by a marked decrease in the insulin-like growth factor 1 (IGF1) and IGF1-receptor (IGF1R) expression. The underlying mechanism remains unexplored. This study examined the role of microRNAs in post-natal cardiac remodeling. By expression profiling, we observed a 10- fold increase in miR-378 expression in 1 wk old neonatal mouse hearts compared to 16th day old fetal hearts. There was also a 4 to 6-fold induction in expression of miR-378 in older (10 month) compared to younger (1 month) hearts. Interestingly, tissue distribution analysis identified miR-378 to be highly abundant in heart and skeletal muscle. In the heart, specific expression was observed in cardiac myocytes, which was inducible by a variety of stressors. Over-expression of miR-378 enhanced apoptosis of cardiomyocytes by direct targeting of IGF1R and reduced signaling in Akt cascade. The inhibition of miR-378 by its antimiR protected cardiomyocytes against H_2O_2 and hypoxia-reoxygenation induced cell-death by promoting IGF1R expression and downstream Akt-signaling cascade. Additionally, our data show that miR-378 expression is inhibited by IGF1 in cardiomyocytes. In tissues such as fibroblasts and fetal hearts, where IGF1 levels are high, we found either absent or significantly low miR-378 levels, suggesting an inverse relationship between these two factors. Our study identifies miR-378 as a new cardio-abundant microRNA which targets IGF1R. We also demonstrate the existence of a negative feedback loop between miR-378, IGF1R and IGF1 that is associated with post-natal cardiac remodeling and with the regulation of cardiomyocyte survival during stress.

MicroRNAs (miRNAs) are endogenous, small non-coding RNAs that have emerged as powerful negative regulators of gene expression. By targeting specific mRNAs mostly in the 3' un-translated regions, miRNAs either destabilize

target mRNAs and / or inhibit their translation. Bioinformatics predicts that almost 30% of all human mRNAs are regulated by miRNAs(1,2). Recently these regulatory molecules have been suggested to be involved in several biological processes ranging from development and metabolism to apoptosis and signaling pathways. Among the almost 1000 human miRNAs described so far, only a handful are found to be abundant in the heart, such as miR-1, miR-133, miR-208a, miR-208b and miR-499. These cardio-abundant miRNAs have been shown to play fundamental roles in regulating development as well as disease processes (3).

Recent emerging data indicate that miRNAs also play a role in the cardiac remodeling that occurs during the postnatal period. Global inhibition of miRNA processing by cardiac specific deletion of Dicer was shown to cause post-natal lethality from progressive heart failure (4). Cardiac specific conditional deletion of Dicer in the myocardium after birth was also shown to produce spontaneous cardiac remodeling, and cardiac dysfunction resulting in premature death within 1 week (5). More recently, an elegant study from Olson's group demonstrated that the loss of the proliferative potential of cardiomyocytes after birth is related to the up-regulation of miR-15 family members. Knockdown of a single member of this family, miR-195, was sufficient to increase the number of mitotic cardiomyocytes and de-repress Check1(6).

Another important aspect of cardiac remodeling during the post-natal period is the regulatory role played by the insulin-like growth factor 1 (IGF1), a key survival factor in the heart. It is released into the bloodstream by the liver, or synthesized locally by muscles and neural cells. Acting in an autocrine or paracrine fashion, IGF1 via the IGF1R triggers a signaling cascade that plays many essential regulatory roles in multiple aspects of cardiac biology. During the post-natal period, the switch in cardiac metabolism and the cardiomyocyte's withdrawal from the cell cycle is characterized by a marked decrease in the expression of IGF1 and IGF1R (7,8). The down-regulation of IGF / IGF1R is also observed in other organ systems, such as the brain (9). The mechanism of IGF1R down regulation has not yet been described.

In this study we demonstrate that postnatal repression of cardiac IGF1R is associated with the up-regulation of miR-378. Our data illustrate the high abundance of miR-378 in the heart and its stress inducible and specific expression in cardiomyocytes. We found that miR-378 promotes cardiomyocyte apoptosis by directly targeting IGF1R and consequently inhibiting IGF1 mediated activation of Akt. In addition, ligand IGF1 was found to act as an inhibitor of miR-378 expression. Indeed IGF1 abundance correlated with the depression of miR-378 in cardiac fibroblasts in culture, and in vivo in the fetal heart and vice versa after birth. Together, our findings define a functional role of miR-378 in the heart and unravel a unique reciprocal molecular circuit between miR-378, IGF1R and IGF-1, which appears to play a significant regulatory role during post-natal cardiac remodeling.

Experimental Procedures

Reagents and Antibodies: Reagents used in the study were purchased as follows: Dulbecco's modified Eagle's medium (DMEM), Lipofectamine 2000, TRIZOL, T4 DNA ligase, Restriction enzymes, Superscript III reverse transcriptase kit, DH5α cells, RNA oligos (378-mimic, 378-antimiR, scramble and mimic control), OPTIMEM transfection media and Lipofectamine were purchased from Invitrogen; Fetal Bovine Serum (FBS) from Gemini Inc.; collagenase type 3, trypsin and soybean inhibitor from Worthington Biochemicals; DNA probes for miR1, miR-378, miR-378*, miR-133a, U6 and miR-208a were synthesized from IDT; Gel extraction kit and DNA Maxi prep kit from Qiagen; Fast SYBR Green Master Mix was from Applied Biosystems; ECL Western blot detection kit, chemiluminescence films and Nylon membrane HyBond N+ were purchased from Amersham, GE Healthcare; Nitrocelulose transfer membrane, RC/DC assay and Precision Plus Dual protein ladder were from BioRad; Restore Western blot stripping buffer was from Thermo Sci.; PQ401, Horseradish peroxidase conjugated anti rabbit antibody, laminin, and other general chemicals were purchased from Sigma Chemicals; Hybridization buffer and Nuc

Away columns from Ambion; In Situ Cell Death (TUNEL) detection kit was from Roche; pmiRGLO vector, Caspase-Glow assay, ApoTox Glo Triplex Assay kit and Dual Luciferase assay kit were purchased from Promega and p^{32} γATP from Perkin-Elmer. Specific antibodies were obtained from following sources: Akt, anti p-Akt (Thr308 and Ser478), pERK, Foxo3, p-Foxo3a and p-IGF1R β were purchased from Cell Signaling; FasL, TRAIL, Bim, GAPDH, ERK2, β-actin, HRP conjugated anti-mouse or anti-goat antibodies were from Santa Cruz; anti-human Insulin like growth factor-I and anti-rabbit HRP antibody were from Sigma; IGF1R (β subunit) antibody from Milipore; α actinin and phospho-ERK1/2 were from Abcam Inc.; fluorescent labeled Alexa Fluor 488 (green) and 594 (red) antibodies, ToPro nuclei labeling reagent and ProLong Gold antifade reagent were purchased from Molecular Probes.

Animals: All animal experiments were performed in accordance with currently prescribed guidelines and under a protocol approved by the Institutional Animal Care and Use Committee at University of Illinois at Chicago.

Cell culture: Primary cardiomyocyte cultures were isolated from one day old neonatal rats (Sprague Dawley, Harlan Co.) as per our published procedures (10). For experiments requiring non-muscle cells, cells were obtained during the pre-plating step and cultured for appropriate density. H9C2 cells were grown in DMEM supplemented with 10% FBS. Seventy two hr prior to transfection, cells were switched to differentiation media (DMEM + 2% FBS) and maintained in this medium throughout experimental period.

Northern analysis: Total RNA was isolated using TRIZOL reagent and 10-20 ug of total RNA resolved in 12% UREA PAGE, transferred onto HyBond N+ nylon membrane by electro blotting in 0.5x TBE buffer (89mM Tris base, 89mM Boric acid,2mM EDTA). Pre-hybridization for 2 hr at 42^0C and hybridization in presence of p32γATP labeled specific oligo probe overnight was carried out in hybridization buffer. The membranes were washed in 2xSSC buffer (150mMNaCl, 15mM Na3Citrate X 2H2O). Images were captured by exposing to the Phospho imaging screen followed by scanning on a Storm 860 scanner. Signals were quantified using Image J program. U6 labeled radioactive probe was used as control for all samples after membranes were stripped in 1x SSC/0.1%SDS buffer at 72^0C.

Western analysis: Cell lysates were prepared in Urea-Thiourea sample buffer (8M urea, 2M thiourea, 0.05MTris pH6.8, 75mMDTT, 3%SDS, 0.05%bromphenol blue) by brief sonication, protein concentrations determined by RC/DC protein assay kit and equalized proteins were resolved by SDS PAGE gel (30 ug/lane unless otherwise indicated). Western blotting was performed using standard protocols. Each membrane was stripped and re-probed with either GAPDH or β-actin primary antibody for loading control. Signal intensities were quantified using Image J 1.37v software (NIH).

Caspase 3/7 activity assay: Caspase activity was measured by luminescent assay for caspase 3/7 detection as per manufacturer instructions in a 96 well plate format. Signal was measured at 491 nm using a Promega luminometer micro plate reader. Values are expressed as relative light units (RLU, blank subtracted).

DNA fragmentation by TdT mediated dUTP nick end labeling (TUNEL) staining and viability assay: Cardiomyocytes were grown on glass coverslips. After 72 hr of transfection, cells were permeabilized and TUNEL reaction performed as per manufacturer's instructions. With each assay run, a negative control (by omitting dUTP or TdT) was included. TUNEL positive cells were identified by fluorescence microscopy using an excitation wavelength of 488 nm. Cells were defined as apoptotic when the TUNEL (green) labeled nuclei were detected with a sharply demarcated and condensed morphology. To-Pro reagent was used for nuclei visualization, according to manufactures protocol. For quantitative data expression, TUNEL positive nuclei were counted from 10 random fields with 30-50 nuclei per field and average values calculated from 20 different images in each group. . Cell viability was measured by MultiTox-glo Assay kit (Promega) as per manufacturer.

Simulated Ischemia/Reperfusion Treatment: To simulate in vivo I/R conditions, 48 h after transfections, cardiomyocytes were exposed to hypoxia and oxygenation as was described

previously (11). Briefly, cells plated in DMEM complete medium were placed in a Plexiglas chamber, and exposed to a constant stream of water-saturated 2% O_2, 93% N_2, and 5% CO_2 for indicated time. Maintenance of the desired O_2 concentration was constantly monitored during incubation using a microprocessor-based oxygen sensor. Following exposure to hypoxia, the cells were re-oxygenated in a humidified tissue culture incubator with 5% CO_2-95% air. For the inhibitor experiments, the IGF-1R inhibitor PQ401 was added 30 minutes prior to the exposure of hypoxia.

Immunofluorescent staining and confocal microscopy: Cardiomyocytes were grown on glass coverslips and processed for confocal microscopy according to our published procedures (12) using FoxO3 primary antibody and additionally with α actinin antibody for myocyte visualization. Cells were then washed and incubated with fluorescently labeled Alexa Fluor 488 and Alexa Fluor 568 conjugated antibodies. Nuclei were visualized by ToPro reagent as per manufacturer's protocol. Cells were washed and mounted on glass slides using ProLong Gold antifade reagent. Imaging was performed on a Bio-Rad Laser Sharp 2000 system (Bio-Rad) using a 40x objective (Zeiss). For each experimental group, there was a minimum of three experiments with at least three replicates of each sample.

Dual luciferase reporter assay: Firefly and Renilla luciferase activities were measured sequentially using a Dual Luciferase Reporter Assay System as per manufacturer's instructions. The firefly luciferase signal was measured first at 480nm and followed by Renilla luciferase at 560nm in the same sample using a EG&G Berthold LUMAT LB9507 reader. Firefly luciferase activity was normalized by Renilla luciferase signal and values expressed as arbitrary relative light units.

DNA constructs and cell transfection: A three repeat sequence of miR-378 predicted target region was synthesized from the 3'UTR of human IGF1R and cloned into an Xho-Xba site in a dual luciferase reporter vector pmiRGLO. Control construct with mutations incorporated in the miR-378 seed region was generated similarly. These constructs were sequence verified. Cells were transfected with various DNA constructs and RNA oligos using OPTIMEM and Lipofectamine2000 as per manufacturer's protocol. All transfections were performed in triplicate in 3 independent experiments.

Real-time polymerase chain reaction: Total RNA was isolated and treated with DNase I to eliminate residual genomic DNA. MicroRNAs expression profiling was performed according to the method described by (13). Briefly, a multiplex cDNA reaction was carried out where 1 μg of total RNA was primed by a pool of 24 oligo nucleotides and reverse transcribed using Superscript III reverse transcription reagent. Real-time amplification of individual microRNAs was then performed in a SybrGreen based assay reaction using a Fast ABI cycler and microRNA specific F and R primers. U6 was used as a normalizing control. Real-Time PCR primers for mouse *Igf1R* and *Pgc1β* were designed using Real-Time PCR Primer Design (//www.genscript.com/ssl-bin/app/primer), and the sequence is available upon request. 2.5 ug of DNase-digested total RNA was reverse transcribed using the SuperScript III kit and random hexamers. In a 20 ul PCR reaction, 5 ng of cDNA template was mixed with primers to a final concentration of 200 nM and 10 ul of Fast SYBR Green master mix. Amplification was carried out in a 7500 Fast Real-Time PCR system by first incubating the reaction mix at 95° for 20 s, followed by 40 cycles of 95° for 20 s and 60° for 30 s. For quality control purposes, at the end of each run, dissociation curves were generated by incubating the reactions at 95° for 15 s, 60° for 1 min, 95° for 15 s, and 60° for 15 s. Primer pairs used in the study were free of primer dimer artifact. Expression ratios were calculated by the $\Delta\Delta C_T$ method, where C_T is the cycle threshold, using β-actin as a reference gene.

Statistical analysis: Data are expressed as the mean and the standard deviation (SD) of at least three independent experiments. Control and treatment groups were matched in sets containing cells isolated and cultured on the same day to eliminate variability due to a cell batch. The two-tailed student's T test was used for performing analysis of variance in Excel software. A *p* value of 0.05 or less was considered statistically significant.

RESULTS

Several microRNAs are induced in heart after birth: Real-time qPCR of 23 randomly selected microRNAs showed increased expression of 8 microRNAs by 4-fold or more in mouse neonatal heart (7 days after birth) when compared to fetal hearts at 16 day gestation. Among these, expression of miR-1, miR-133, miR-208a and miR-378 was found to be increased by more than 10-fold (Figure 1A). The findings were verified by Northern analysis (Figure 1B) which also showed different kinetics of induction after birth (Supplement Figure1A), suggesting their differential roles in post-natal cardiac remodeling.

High abundance and cardiomyocyte specific expression of miR-378 in the heart: Several previous studies have suggested that miR-1, miR-133a and miR-208a are abundantly expressed in the heart and play regulatory roles in various aspects of cardiac patho-physiology, but the role of miR-378 in the heart has never been investigated. We got interested in miR-378 because it is not only induced during post-natal period, but is also derived from the *Pgc1β* gene which has been shown to play critical roles in regulating cardiac cell metabolism(14). The first intron of the *Pgc1β* gene contains a stem loop structure which gets processed into two microRNAs; miR-378 and miR-378* (Figure 1C). We first performed a tissue distribution analysis and found that miR-378 is highly expressed in heart and skeletal muscles, low levels were found in kidney, liver, and small intestine, minimal in spleen and uterus, and none in the lung (Figure 1D, Supplemental Figure 1B). We next examined the relative expression of miR-378* by stripping and re-probing the same membrane and found very weak cardiac expression of miR-378*. We also examined miR-378* in the fetal and the neonatal heart and found that it is not inducible after birth (Figure 1D). Therefore this study focused on miR-378 for further characterization in the heart. Intriguingly, miR-378 was found expressed only in the cardiac myocytes and not in non-muscle cells obtained during the pre-plating step of the same culture (Figure 1E). We even used 3 times more RNA amount than that was used for cardiac myocytes and still did not find miR-378 in non-muscle cells, treatment of these cells with Angiotensin II, a well-known stimulator of fibroblast cell proliferation, also did not induce miR-378 (data not shown). Additionally, we observed that cardiac expression of miR-378 increased continuously as animals aged from 4 wks to 6 months and further onto 10 months (Figure 2A). Next, we examined if the age related increase in miR-378 originates from its induction in aging fibroblasts, by culturing fibroblasts from the aged hearts and again found no expression (not shown), suggesting that age-related increase of miR-378 occurs in the cardiomyocytes.

Up-regulation of miR-378 by stress: One of the characteristic features of the aged myocardium is its greater susceptibility to stress-related injuries. Since miR-378 showed an age related increase in expression, we asked whether it responds to stress inducing agents. Cardiomyocytes were treated with camptothecin, which induces cell stress by inhibiting DNA topoisomerase (15), or with H_2O_2 - a well-known inducer of oxidative stress. Camptothecin and higher doses of H_2O_2 significantly enhanced miR-378 expression (Figure 2B and 2C). In contrast, growth promoting stimuli such as serum and α-adrenergic receptor agonist, phenylephrine (not shown) had no effect on miR-378 expression. We also examined the influence of nutrient stress on miR-378 and found that cardiomyocytes grown in low glucose (2 mM or 5 mM) media had almost a 3-fold higher expression as compared to control media (25 mM glucose). The expression of the miR-378 precursor or the unrelated microRNA, miR-208a, was not influenced by any of the tested stressors. To probe into the mechanism of this stress related induction of miR-378 expression, we examined the mRNA levels of its parent gene *Pgc1β* in the same RNA preps and found a similar pattern of induction (Figure 2D). Taken together, our results indicate that miR-378 is a stress-responsive miRNA in cardiac myocytes whose expression is co-induced with its parent gene by stressors.

IGF1R is an endogenous target of miR-378 mediated repression: Using a bioinformatics approach, we searched for candidate miR-378 targets among genes that are known to be down-

regulated during post-natal cardiac remodeling. We used prediction tools, TargetScan (www.targetscan.org) and Microcosm Targets (www.ebi.ac.uk/enright-srv/microcosm/cgi-bin/targets/v5/detail_view.pl?transcript_id=ENST00000268035), and both identified a match of a miR-378 'seed' sequence along with the flanking nucleotides within the 3'UTR of IGF1R. This region was found highly conserved across several vertebrate species (Figure 3A).

The IGF1R is comprised of two alpha subunits and two beta subunits. Both α-and the β-subunits are synthesized from a single mRNA precursor. The α-chains are located extracellularly whereas the β subunits span the membrane and are responsible for intracellular signal transduction upon ligand stimulation. Using an antibody against the β subunit of IGF1R, we first examined the relationship between the expression level of IGF1R and miR-378 (Figure 2A and 3B) in 16th day-fetal hearts vs. 1wk, 2wk, 4wk and 10 months after birth and observed an inverse relationship between miR-378 expression and IGF1R protein levels at all-time points (Figure 3C). This was also evident in fibroblasts where IGF1R is highly expressed, consistent with previous reports(16), whereas expression of miR-378 is not detected in cardiac fibroblasts (Figure 1E). The inverse expression pattern suggested that IGF1R could serve as a target gene for miR-378. For experimental validation, gain-in-function studies of miR-378 for endogenous IGF1R were performed in cardiomyocytes. For overexpression, a synthetic, commercially available double stranded miR-378-mimic (378-mimic) was used. For controls, a double stranded mimic control designed with no homology to any of the miRNA sequences available in the mouse, rat or human miRNA database was used. Transfection of primary cultures of cardiomyocytes with 25nM and 50nM of 378-mimic resulted in 10-fold and 15-fold higher expression of mature miR-378 with no effect on its precursor level (Figure 4A). Western analysis showed a dose dependent decline in IGF1R expression by 30% and 52% with 25nM and 50nM 378-mimics (Figure 4B). A comparable decline in IGF1R expression in 378-mimic transfected cells was also observed when we compared it against an additional control group where cells were transfected with a custom RNA oligo with mutated seed region of miR-378 (not shown). We also evaluated *IGF1R* mRNA by real-time PCR and found no change with 378-mimic (Figure 4C). Taken together our data suggest that miR-378 produces translation inhibition and not the mRNA stability of IGF1R.

We next evaluated whether the predicted 3'UTR sequence of *IGF1R* could be targeted by miR-378 in a luciferase-3'UTR functional assay. To eliminate the influence of endogenous miR-378 targeting luciferase reporter, we first utilized cardiac fibroblasts, which do not express miR-378, but these cells could not survive with 378-mimic transfection. Subsequently, we analyzed miR-378 expression in H9C2 cells, a cell line derived from embryonic rat heart. Consistent with low expression level of miR-378 in fetal heart, the H9C2 cells were found to express very low levels of miR-378, we had to use 3X more RNA than from fetal heart to detect a minimal miR-378 signal (not shown). Co-transfection of *wtIGF1R-luc* with 378-mimic resulted in a dose-dependent reduction in luciferase activity whereas mimic control had no effect. There was no effect on luciferase reporter, when 378-mimic was co-transfected with empty vector or with *mutIGF1R3X-luc* (with mutated *IGF1R* 3'UTR sequence) (Figure 4D). The incorporated mutation significantly disrupted miR-378 seed region to form a hybrid as shown (Supplemental Figure 2) with increased minimum free energy from -27.5 kcal/mol (WT IGF1R / miR378 hybrid) to -10.7 kcal/mol (mutant *IGF1R* / miR-378 hybrid). Taken together, these results suggest *IGF1R* 3'UTR as a bona fide miR-378 target.

It has been demonstrated that IGF1/IGF1R signaling involves activation of PI-3 kinase, the serine-threonine kinase Akt and ERK1/2 (17). To examine the influence of miR-378 on IGF1 induced cardiac response cardiomyocytes were either mock transfected, transfected with mimic control or with 378-mimic (25 and 50 nM) in duplicates. After 48 h, cells were serum starved overnight, one set of plates was treated with IGF1 (10 nM) the other received vehicle for 15 min. IGF1 caused Akt activation (Thr-308) which was comparable in mimic control and

mock-transfected cells (not shown). Transfection of 378-mimic on the other hand produced a dose-dependent decline in Akt and ERK activation by IGF1 (Figure 5A and 5B). In contrast, when cells were treated with phenylephrine there was no inhibition in pERK rather an increase was observed with 378-mimic compared to mimic control group (Figure 5C). It is therefore apparent from these findings that miR-378 specifically targets IGF1R mediated signaling. To further establish a link between miR-378 and IGF1R mediated signaling we used a specific inhibitor of IGF1R, N-(5-Chloro-2-methoxyphenyl)-N′-(2-methylquinolin-4-yl) urea, also known as PQ-401 which is shown to suppress IGF1 stimulated auto-phosphorylation of IGF1R with IC_{50} of 12 uM (18). Cardiomyocytes were transfected and serum starved as above in duplicates, after 48h, one set of plates was treated with PQ-401 and the other with vehicle for 90 min followed by IGF for 15 min. As shown in Fig.5D, the inhibition of pAkt by PQ401 was augmented by miR-378. PQ401 produced about 48% reduction in pAkt in mimic control group whereas it produced 62% and 75% reduction when combined with 10nM and 25nM 378-mimic as compared to non-treated 378-mimic transfected cells. The compounded effect of PQ-401 with miR-378 over-expression further suggest that this microRNA acts as a repressor of IGF1R.

Expression of miR-378 sensitizes cardiomyocytes to cell-death stimuli: Activated Akt is a well-known survival signal in cardiomyocytes particularly during stress. Data presented in Figure 2 show that miR-378 is a stress responsive microRNA and those in Figure 5 demonstrate that over-expression of miR-378 reduces pAkt. With this in mind, we examined the influence of 378-mimic on cardiomyocyte apoptosis induced by H_2O_2. Primary cultures of cardiomyocytes were either mock transfected, with mimic control or with 378-mimic. Evaluation of DNA fragmentation showed that 4h treatment with H_2O_2 produced a 2 to 2.5-fold more increase in TUNEL positive nuclei with 378-mimic as compared to mimic control or mock transfected cells (Figure 6A, 6B). Caspase 3/7 activity following different durations and doses of H_2O_2 treatment in cardiomyocytes was also found to be significantly higher with 378-mimic at all data points (Figure 6C). More importantly, at suboptimal doses of H_2O_2 (200uM, 18 hr) when there was no caspase activation in control groups, over-expression of miR-378 resulted in twice as much caspase activation as observed in mock or mimic control transfected cells. We next evaluated apoptosis inducing signaling cascade by examining the expression of FoxO3 and its transcriptional targets such as Bim, Trail and FasL in the presence of 378-mimic or mimic control. As shown in Figure 6D and 6E, along with the reduced expression of pIGF1R, IGF1R and pAkt, 378-mimic also produced significantly lower levels of pFoxO3 accompanied by increased expression of Bim, Trail, and FasL (Figure 6D and 6E). These findings collectively suggest that enhanced expression of miR-378 makes cardiomyocytes more susceptible to caspase activation and DNA fragmentation in response to stress inducing agents, consistent with increased cell death. This may have an in vivo implication in imparting greater susceptibility of the aged myocardium (where miR-378 is found increased) to stress related injuries.

Inhibition of endogenous miR-378 induces IGF1R and pAkt levels: We also took a complementary approach where we knocked-down miR-378 in cultured cardiomyocytes and evaluated Akt activation by IGF1. The knocked-down of miR-378 was achieved by a commercially available miR-378 antimiR and verified by Northern analysis (Figure 7A). For controls, we used a single stranded scramble oligo, which was designed not to target any known miR sequences. Evaluation of IGF1R expression by Western showed about 2 to 2.5-fold induction with 378-antimiR in relation to scramble control group (Figure 7B). The pAkt levels by IGF1 activation were also found significantly higher (9 to 10-fold) in 378-antimiR group than scramble control group (only 5 fold-induction) in relation to corresponding non-treated cells (Figure 7C). To analyze role of IGF1R in 378-antimiR mediated enhancement of Akt activation, we performed same experiment but in presence of IGF1R inhibitor, PQ-401. As shown in Figure 7D 378-antimiR antagonized the inhibition of pAkt caused by PQ-401. The role of IGF1R signaling

in 378-antimiR mediated Akt activation was also evident when we used combined inhibition of IGF1R and down-stream PI3K, the 378-antimiR again minimized the effect of these inhibitors on Akt activation (Supplemental Figure 3). Taken together our results support that knock-down of miR-378 enhances IGF1R and its mediated signaling.

Inhibition of miR-378 prevents H_2O_2 induced activation of apoptosis signaling cascade and hypoxia/reoxygenation induced DNA damage in IGF1R dependent manner: Several groups have shown that one of the mechanisms by which pAkt promotes cell survival under conditions of stress is by phosphorylating the FoxOs, promoting their nuclear exportation and thereby inhibiting their ability to induce the apoptosis gene program (19). We examined 378-antimiR in the context of pFoxO and its down-stream apoptosis inducing signaling cascade, such as Bim, Trail and FasL in cardiomyocytes following H_2O_2 treatment (500uM, 4h). As shown in Figure 8A and 8B, 378-antimiR not only induced the expression levels of pIGF1R, IGF1R, pFoxO3, but it significantly reduced the expression of Bim, Trail and FasL. We also tested 378-antimiR in another oxidative injury model of hypoxia-reoxygenation. As shown in Figure 8C and Supplemental Figure 4, sequential exposure of cardiomyocytes to hypoxia and re-oxygenation for increasing duration (2h, 3h and 4h) increased the number of TUNEL positive nuclei in mock transfected cells which was similar to scramble control group. Transfection of 378-antimiR drastically reduced cell death at each time point such that at 4h of hypoxia followed 4h re-oxygenation, there was almost 75% reduction in the number of TUNEL positive nuclei in 378-antimiR group compared to scramble control. To examine the involvement of IGF1R in 378-antimiR mediated cardio-protection, cells were transfected as above with scramble or 378-antimiR for 48h and then exposed to varying amounts of PQ-401 for 90 min followed by 2h hypoxia and 2h reoxygenation. As shown in Figure 8D, 8E and supplemental Figure S5 presence of PQ-401 antagonized the 378-antimiR mediated cardioprotection both on viability as well as on number of TUNEL positive cells. These results suggest that IGF1R plays a critical role in 378-antimiR mediated inhibition of cell death.

We also examined whether 378-antimiR would influence the subcellular distribution of FoxO3 under oxidative stress induced by H_2O_2 (500uM, 4h). Confocal microscopy was used to visualize FoxO3 distribution in co-cultures of cardiac myocytes and cardiac fibroblasts. Our reason for using co-culture for this particular experiment was related to the myocyte-specific expression of miR-378 (Figure 1E). Therefore, following oxidative stress one would expect to see interference of nuclear presence of FoxO3 in myocytes and not in non-muscle cells. Myocytes were identified by counter staining with α-actinin. As shown in Figure 9A, under basal non-treated conditions, transfection of cells with scramble or 378-antimR did not change FoxO3's distribution in muscle or in non-muscle cells. But when these cells were treated with H_2O_2, in scramble control group nuclear translocation of FoxO3 was observed in both muscle as well as in non-muscle cells, in contrast, with 378-antimiR transfection FoxO3 immuno-fluorescence was not detected in nuclei of α-actinin positive (muscle) cells whereas non-muscle cells showed nuclear FoxO3. Together these results indicate that in the presence of oxidative stress, 378-antimiR interferes with FoxO3 mediated induction of the apoptosis signaling cascade preferentially in cardiomyocytes.

IGF1 acts as a negative regulator of miR-378: We also examined if miR-378 plays a role in down-regulation of IGF1 seen during post-natal period (Figure 9B). For this cardiomyocytes were either mock transfected or with mimic control or 378-mimics, and the cell lysates analyzed for IGF1 expression by Western. As shown in Figure 9C and supplemental Figure S6, although lower expression of IGF1 was noted when 378-mimic group was compared with mimic control group the difference did not reach statistical significance. The IGF1 expression was significantly different between two controls (mock and mimic control cells). We next asked whether IGF1 which is a ligand for IGF1R would regulate the miR-378 expression. For this, cardiac myocytes were treated with increasing doses of IGF1 (10 and 50nM) for 48h

and miR-378 expression was evaluated by Northern. IGF1 caused a dose-dependent reduction in miR-378 expression (Figure 9D). These results together indicate that miR-378 does not influence IGF1's expression significantly but IGF1 acts as an inhibitor of miR-378 suggesting that the high levels of IGF1 before birth could be contributing to the reduced level of miR-378 observed in the fetal heart.

DISCUSSION

It has been long appreciated that the IGF1/IGF1R system is down-regulated during the maturation of the heart after birth, which appears to be coupled to the attenuation of cardiomyocytes proliferation and to the reduced uptake and metabolism of glucose by cardiomyocytes. The underlying mechanism of IGF1/IGF1R down-regulation remains unknown. In this study we provide the first evidence of down-regulation of IGF1R in cardiac myocytes by miR-378. The data supporting this conclusion are as follows: First, cardiac expression of miR-378 is significantly lower in the fetal heart and induction of miR-378 after birth paralleled with the diminution of IGF1R expression starting 1 wk after birth and continuing thereafter. Second, a highly conserved target sequence of miR-378 is present in the 3'UTR of *IGF1R*. When cloned downstream of the luciferase reporter, this sequence led to the reduced luciferase activity in the presence of miR-378. Third, when over-expressed, miR-378 reduced the expression level of endogenous IGF1R without influencing IGF1R mRNA stability, whereas inhibition of miR-378 by 378-antimiR resulted in the increase endogenous level of IGF1R beyond normal. From these data it is apparent that IGF1R is a direct target of miR-378, and that up-regulation of miR-378 after birth could contribute to the post-natal repression of IGF1R.

It is known that miR-378 is the product of the guide strand of a miRNA hairpin located in the first intron of *Pgc1β*, the complementary strand of which also has the potential of processing into miR-378*. We found that in the heart, miR-378 is the predominant species while expression level of miR-378* is minimal. This is in contrast to a breast cancer cell line, BT-474, where both miR-378 and miR-378* mature forms were equally detected following transfection with pre-miR-378 (20) suggesting cell type specificity in the processing of 378-premiR. Cell-type specific processing of miR-378 is also suggested by our data where we detected mature form of miR-378 only in cardiomyocytes and not in non-muscle cells whereas pre-miR expression was equally detected in both type of cells. In addition, our tissue distribution analysis of miR-378 also showed comparable or in some tissues even higher levels of 378-premiR expression, yet, mature form of miR-378 was predominantly observed only in striated muscles, further supporting the role of tissue-specific factors in processing of 378-premiR. A recent study also suggested cell type specific factors in eliciting transactivation of miR-378 by c-Myc, and its oncogenic potential in c-Myc-driven cell transformation (21). Our finding of induced miR-378 expression during the post-natal period suggests that processing of 378-premiR in the heart is also subject to regulation by developmental factors. Previously, in carcinoma cell lines U87 and MT-1 as well as in pooled cells, transfection of 378-premiR hairpin was reported to promote tumor growth and angiogenesis. This study showed miR-378* seed sequence (addressed in this report as miR-378) to target transcription factors SuFu and Fus-1 (22) and promote cell survival, whereas in our study we observed apoptosis inducing role of miR-378 in cardiomyocytes. Additionally, miR-378* has been shown to promote metabolic switch from OXPHOS to glycolysis in a BT-474 breast cancer line (20). The role of miR-378 was not investigated in this study. The findings of our study demonstrating miR-378 directly targeting IGF1R (which is known to promote glucose uptake and metabolism) suggest that miR-378 may also have a role in metabolic switch that occurs in the post-natal heart. If so, miR-378 must work in collaboration with its parent gene which is known to stimulate the expression of genes involved in OXPHOS metabolism rather than in the contradictory manner as was seen for miR-378* in BT-474 breast cancer cell line. This speculation needs to be examined in future experiments.

Previous studies have shown that cardiac myocytes possess IGF1R and are also capable of synthesizing and secreting IGF1. The local IGF1/IGF1R system plays a regulatory role in cardiomyocyte growth and survival. In transgenic mice, cardiac specific over expression of IGR1R triggered myocyte hypertrophy and enhanced systolic function (23). IGF1R signaling is also found to be essential in inducing physiological growth associated with exercise induced cardiac hypertrophy (24). Exogenous administration of IGF1 in vivo reduces cardiomyocyte apoptosis in response to stress injury (25-28). Intriguingly, genetic studies conducted in murine models indicate that an excess of IGF1 signaling may also trigger cardiac dysfunction (29). This emphasizes the importance of gaining a better understanding of the mechanisms controlling IGF1/IGF1R regulation and gene transcription.

We show that miR-378 targets IGF1R and the ligand IGF1 acts as a negative regulator of miR-378. This is evident in vitro as treatment of cardiomyocytes with IGF1 reduced the expression of endogenous miR-378. In vivo, we observed a negative correlation between high levels of IGF1 with reduced levels of miR-378 in fetal heart and no expression in fibroblasts. Thus, our study provides evidence of the existence of a feedback loop where miR-378 is reducing the expression of IGF1R and the ligand IGF1 is inhibiting miR-378. Our findings show that miR-378 does not significantly affect IGF1 expression in cardiomyocytes. Previous studies have shown miR-1 as a repressor of IGF1 and IGF1R in skeletal muscle during differentiation as well as in the heart (30) and down-regulation of miR-1 is linked to IGF1 induction in myocardial infarction (31). We found that miR-1 expression is induced in the heart after birth; therefore it is likely that the repression of IGF1/IGF1R signaling during the post-natal period must be the result of concerted activity of more than one microRNAs in the heart.

The regulation of programmed cell death is crucial to the normal physiology of almost all multicellular organisms. Increasing evidence demonstrates that apoptosis contributes to tissue injury in several cardiac disorders including myocardial infarction, atherosclerosis, myocarditis, cardiac failure, and during cardiac transplantation. In rodent and humans it is shown that about 5% to 30% of cardiac myocytes undergo apoptosis within hours of reperfusion injury (32-36), and higher apoptosis can be observed even after several months of ischemic insult (37,38). Genetic approaches using rodents have determined that inhibition of apoptosis in cardiac myocytes reduces infarct size by more than 50% (39,40). In line with these reports, short-term treatment with IGF-1, and cardiomyocyte specific transgene expression of IGF1 has been reported to improve cardiac function and counteract the occurrence of apoptosis in experimental myocardial infarction and in a murine model of heart failure (41,42). Since IGF1 is a well-accepted survival factor, our data suggest that one of the mechanisms by which IGF1 protects cardiomyocytes may involve its ability to inhibit miR-378, thereby enhancing the expression of its receptor to trigger cell survival signals. This is evident from our data, which showed that during oxidative stress induced by H_2O_2 and by simulated ischemia / reperfusion injury, elimination of miR-378 by 378-antimiR led to enhanced cell survival by promoting IGF1R and pAkt expression and reducing levels of apoptosis inducing factors, Bim, Trail and FasL. Interestingly, in line with our observation of cardiomyocyte specific expression of miR-378, we observed that following H_2O_2 challenge, inhibition of miR-378 resulted in cytoplasmic retention of FoxO3 only in cardiomyocytes whereas the nuclear presence of FoxO3 was detected in non-muscle cells in the same culture. Therefore it would be possible to promote cardiomyocyte survival with 378-antimiR implicating its therapeutic potential in conditions of ischemic injury where cardiomyocyte apoptosis contributes significantly to the disease process.

During the embryonic period, IGF1/IGF1R signaling is associated with the proliferation of cardiac myocytes. In cultures, stimulation of IGF1/IGF1R system is known to activate DNA synthesis in neonatal cardiomyocytes (43) and to promote cell cycle progression and cell proliferation in fibroblasts (16). The antisense inhibition of IGF1R markedly attenuates cell proliferation (8). Although we have not examined the influence of

miR-378 on cell proliferation or cell cycle progression, our finding of induction of miR-378 during the post-natal period suggests that similar to miR-195, which is also induced in the post-natal heart and suppresses cardiac cell proliferation (6), miR-378 may exert similar effects by inhibiting IGF1R signaling. Another interesting aspect of our finding is the increased miR-378 expression in aged hearts. This would be important since cardiomyocytes isolated from IGF1 transgenic mice show attenuated response of age-related increases in markers of growth arrest and senescence, such as $p27^{kip1}$, $p16^{INK4a}$ p53, and $p19^{ARF}$ (44), suggesting that 378-antimiR may also block such senescence markers by enhancing IGF1R signaling specifically in cardiac myocytes.

Our data presented in this study provide the first evidence of a role of miR-378 in the heart and indicate that 378-antimiR could provide resistance to cardiac myocytes against stress-mediated cell death. Future studies directed towards examining the beneficial effect of miR-378 inhibition in conditions of pathological stresses at the whole organ level will provide further support to the therapeutic potential of 378-antimiR. In addition, such interventions in young vs. old animals are likely to shed more light on its role in age-related susceptibility of cardiomyocyte to stress related injury.

References

1. Lewis, B. P., Burge, C. B., and Bartel, D. P. (2005) *Cell* **120**, 15-20
2. Berezikov, E., Guryev, V., van de Belt, J., Wienholds, E., Plasterk, R. H., and Cuppen, E. (2005) *Cell* **120**, 21-24
3. Small, E. M., and Olson, E. N. (2011) *Nature* **469**, 336-342
4. Chen, J. F., Murchison, E. P., Tang, R., Callis, T. E., Tatsuguchi, M., Deng, Z., Rojas, M., Hammond, S. M., Schneider, M. D., Selzman, C. H., Meissner, G., Patterson, C., Hannon, G. J., and Wang, D. Z. (2008) *Proc Natl Acad Sci U S A* **105**, 2111-2116
5. da Costa Martins, P. A., Bourajjaj, M., Gladka, M., Kortland, M., van Oort, R. J., Pinto, Y. M., Molkentin, J. D., and De Windt, L. J. (2008) *Circulation* **118**, 1567-1576
6. Porrello, E. R., Johnson, B. A., Aurora, A. B., Simpson, E., Nam, Y. J., Matkovich, S. J., Dorn, G. W., 2nd, van Rooij, E., and Olson, E. N. (2011) *Circ Res* **109**, 670-679
7. Cheng, W., Reiss, K., Kajstura, J., Kowal, K., Quaini, F., and Anversa, P. (1995) *Lab Invest* **72**, 646-655
8. Anversa, P., Kajstura, J., Cheng, W., Reiss, K., Cigola, E., and Olivetti, G. (1996) *Cardiovasc Res* **32**, 219-225
9. Torres-Aleman, I., Pons, S., and Arevalo, M. A. (1994) *J Neurosci Res* **39**, 117-126
10. Sulaiman, M., Matta, M. J., Sunderesan, N. R., Gupta, M. P., Periasamy, M., and Gupta, M. (2010) *Am J Physiol Heart Circ Physiol* **298**, H833-843
11. Malhotra, R., Valuckaite, V., Staron, M. L., Theccanat, T., D'Souza, K. M., Alverdy, J. C., and Akhter, S. A. (2011) *Am J Physiol Heart Circ Physiol* **300**, H1733-1742
12. Sundaresan, N. R., Gupta, M., Kim, G., Rajamohan, S. B., Isbatan, A., and Gupta, M. P. (2009) *J Clin Invest* **119**, 2758-2771
13. Wang, X. (2009) *RNA* **15**, 716-723
14. Sonoda, J., Mehl, I. R., Chong, L. W., Nofsinger, R. R., and Evans, R. M. (2007) *Proc Natl Acad Sci U S A* **104**, 5223-5228
15. Hsiang, Y. H., Hertzberg, R., Hecht, S., and Liu, L. F. (1985) *J Biol Chem* **260**, 14873-14878
16. Reiss, K., Cheng, W., Kajstura, J., Sonnenblick, E. H., Meggs, L. G., and Anversa, P. (1995) *Am J Physiol* **269**, H943-951
17. Bueno, O. F., De Windt, L. J., Tymitz, K. M., Witt, S. A., Kimball, T. R., Klevitsky, R., Hewett, T. E., Jones, S. P., Lefer, D. J., Peng, C. F., Kitsis, R. N., and Molkentin, J. D. (2000) *EMBO J* **19**, 6341-6350
18. Gable, K. L., Maddux, B. A., Penaranda, C., Zavodovskaya, M., Campbell, M. J., Lobo, M., Robinson, L., Schow, S., Kerner, J. A., Goldfine, I. D., and Youngren, J. F. (2006) *Mol Cancer Ther* **5**, 1079-1086
19. Ronnebaum, S. M., and Patterson, C. (2010) *Annu Rev Physiol* **72**, 81-94
20. Eichner, L. J., Perry, M. C., Dufour, C. R., Bertos, N., Park, M., St-Pierre, J., and Giguere, V. (2010) *Cell Metab* **12**, 352-361
21. Feng, M., Li, Z., Aau, M., Wong, C. H., Yang, X., and Yu, Q. (2011) *Oncogene* **30**, 2242-2251
22. Lee, D. Y., Deng, Z., Wang, C. H., and Yang, B. B. (2007) *Proc Natl Acad Sci U S A* **104**, 20350-20355
23. McMullen, J. R., Shioi, T., Huang, W. Y., Zhang, L., Tarnavski, O., Bisping, E., Schinke, M., Kong, S., Sherwood, M. C., Brown, J., Riggi, L., Kang, P. M., and Izumo, S. (2004) *J Biol Chem* **279**, 4782-4793
24. Kim, J., Wende, A. R., Sena, S., Theobald, H. A., Soto, J., Sloan, C., Wayment, B. E., Litwin, S. E., Holzenberger, M., LeRoith, D., and Abel, E. D. (2008) *Mol Endocrinol* **22**, 2531-2543
25. Samarel, A. M. (2002) *Circ Res* **90**, 631-633

26. Morales, M. P., Galvez, A., Eltit, J. M., Ocaranza, P., Diaz-Araya, G., and Lavandero, S. (2000) *Biochem Biophys Res Commun* **270**, 1029-1035
27. Ren, J., Samson, W. K., and Sowers, J. R. (1999) *J Mol Cell Cardiol* **31**, 2049-2061
28. Wang, L., Ma, W., Markovich, R., Chen, J. W., and Wang, P. H. (1998) *Circ Res* **83**, 516-522
29. Delaughter, M. C., Taffet, G. E., Fiorotto, M. L., Entman, M. L., and Schwartz, R. J. (1999) *FASEB J* **13**, 1923-1929
30. Elia, L., Contu, R., Quintavalle, M., Varrone, F., Chimenti, C., Russo, M. A., Cimino, V., De Marinis, L., Frustaci, A., Catalucci, D., and Condorelli, G. (2009) *Circulation* **120**, 2377-2385
31. Shan, Z. X., Lin, Q. X., Fu, Y. H., Deng, C. Y., Zhou, Z. L., Zhu, J. N., Liu, X. Y., Zhang, Y. Y., Li, Y., Lin, S. G., and Yu, X. Y. (2009) *Biochem Biophys Res Commun* **381**, 597-601
32. Fliss, H., and Gattinger, D. (1996) *Circ Res* **79**, 949-956
33. Bialik, S., Geenen, D. L., Sasson, I. E., Cheng, R., Horner, J. W., Evans, S. M., Lord, E. M., Koch, C. J., and Kitsis, R. N. (1997) *J Clin Invest* **100**, 1363-1372
34. Olivetti, G., Quaini, F., Sala, R., Lagrasta, C., Corradi, D., Bonacina, E., Gambert, S. R., Cigola, E., and Anversa, P. (1996) *J Mol Cell Cardiol* **28**, 2005-2016
35. Palojoki, E., Saraste, A., Eriksson, A., Pulkki, K., Kallajoki, M., Voipio-Pulkki, L. M., and Tikkanen, I. (2001) *Am J Physiol Heart Circ Physiol* **280**, H2726-2731
36. Wencker, D., Chandra, M., Nguyen, K., Miao, W., Garantziotis, S., Factor, S. M., Shirani, J., Armstrong, R. C., and Kitsis, R. N. (2003) *J Clin Invest* **111**, 1497-1504
37. Guerra, S., Leri, A., Wang, X., Finato, N., Di Loreto, C., Beltrami, C. A., Kajstura, J., and Anversa, P. (1999) *Circ Res* **85**, 856-866
38. Olivetti, G., Abbi, R., Quaini, F., Kajstura, J., Cheng, W., Nitahara, J. A., Quaini, E., Di Loreto, C., Beltrami, C. A., Krajewski, S., Reed, J. C., and Anversa, P. (1997) *N Engl J Med* **336**, 1131-1141
39. Chen, Z., Chua, C. C., Ho, Y. S., Hamdy, R. C., and Chua, B. H. (2001) *Am J Physiol Heart Circ Physiol* **280**, H2313-2320
40. Miao, W., Luo, Z., Kitsis, R. N., and Walsh, K. (2000) *J Mol Cell Cardiol* **32**, 2397-2402
41. Davis, M. E., Hsieh, P. C., Takahashi, T., Song, Q., Zhang, S., Kamm, R. D., Grodzinsky, A. J., Anversa, P., and Lee, R. T. (2006) *Proc Natl Acad Sci U S A* **103**, 8155-8160
42. Welch, S., Plank, D., Witt, S., Glascock, B., Schaefer, E., Chimenti, S., Andreoli, A. M., Limana, F., Leri, A., Kajstura, J., Anversa, P., and Sussman, M. A. (2002) *Circ Res* **90**, 641-648
43. Kardami, E. (1990) *Mol Cell Biochem* **92**, 129-135
44. Torella, D., Rota, M., Nurzynska, D., Musso, E., Monsen, A., Shiraishi, I., Zias, E., Walsh, K., Rosenzweig, A., Sussman, M. A., Urbanek, K., Nadal-Ginard, B., Kajstura, J., Anversa, P., and Leri, A. (2004) *Circ Res* **94**, 514-524

Acknowledgements:

We are thankful to Dr. Shahab Akhtar, University of Chicago, for the use of hypoxia-oxygenation chamber.

Funding:

The study was supported by NIH-Multi P.I. grant 2RO1 HL 22231 (MG and RJS), NIH PO1 HL 062626-Project 1 (RJS), NIH RO1 HL 83423 (MPG) and NIH T32 HL 07692 (IK).

FIGURE LEGENDS

Figure 1: Differential expression of microRNAs in post-natal heart. (A) Expression of randomly selected microRNAs in fetal (16^{th} day gestation) and neonatal (7 day post-natal) mouse hearts by quantitative RT-PCR, asterisks mark p<.05 when compared to fetal heart. (B) Validation of real-time PCR data by Northern analysis (C) Schematic presentation and location of miR-378 in the first intron of *Pgc1β* gene, stem-loop structure of pre-miR-378 and its processing into miR-378 and miR-378* (D) Tissue distribution, and development analysis of miR378 and miR378* by Northern (E) Expression of miR-378 in primary cultures of cardiomyocyte and fibroblasts obtained from the same culture (20ug RNA/lane). Each experiment was repeated a minimum of 3 times. U6 used as loading control.

Figure 2: miR378 is a stress inducible microRNA in rat neonatal cardiomyocytes. (A) Developmental and age-related expression of miR-378 by Northern blotting. (B) Expression of miR-378 following treatment of neonatal cardiomyocytes with various stressors for indicated time and durations. Lower panel shows the expression of a non-related microRNA, miR-208, in the same membrane after stripping and hybridization with radiolabeled miR-208. (C) Quantification of miR-378 normalized to miR-208a, each bar is the mean ± SD of minimum of three independent experiments. (D) Real-time PCR analysis of *Pgc1β* mRNA in the same samples as in B. Relative expression was calculated by ΔΔCT method using β-actin as a reference gene. Asterisks mark the statistical significance ($p<0.05$).

Figure 3: IGF1R as a predicted target of miR-378. (A) Sequence alignment of IGF1R 3'UTR with miR378 seed sequence (highlighted in the box) showing the position of the predicted binding site and species conservation (B) Western analysis of IGF1R in fetal heart and after birth (50ug protein/lane) (C) Inverse expression pattern of miR378 and IGF1R protein levels in cardiac tissues at indicated development time. Blots are representative of a minimum n=3.

Figure 4: miR-378 reduces endogenous IGF1R expression by direct targeting of 3'UTR. (A) Northern analysis showing increased expression of mature miR-378 48 h following transfection of 378-mimic in cardiac myocytes, U6 used as a loading control (B) IGF1R expression by Western in triplicate (50ug protein/lane) in presence of mimic control or increasing amounts of 378-mimic, GAPDH used as a loading control. Graph on the right is derived from 3 additional experiments. (C) Real-time PCR analysis of IGF1R mRNA levels in mimic control and 378-mimic transfected cells (n=2). (D) Functional assay of IGF1R 3'UTR in H9C2 cells using a dual luciferase reporter system following transfection of various DNA constructs in presence of 378-mimic or mimic control. The sequence shown is the predicted target sequence of IGF1R 3'UTR, three repeats of this sequence (WtIGF1R 3X-luc) or mutated sequence (underlined nucleotide mutIGF1R3X-luc) were cloned downstream of luciferase reporter, Renilla luciferase activity was used for normalizing data. Data is derived from triplicate tranfectants of 3 independent experiments.*$p<0.05$.

Figure 5: Inhibition of IGF1 but not PE induced signaling and augmentation of PQ-401 effect on pAkt by miR-378 (A) Western analysis showing pAkt (Thr308) and total Akt in neonatal rat cardiomyocytes following transfection with mimic control or 378-mimic for 48 h, cells were then serum starved overnight and treated with IGF1 (10nM) for 15 min. (B) Same cell lysates as in (A) analyzed for pERK and total ERK2. (C) Cells were prepared as in (A), but treated with phenylephrine (50uM) for 5 min and analyzed for pERK and total ERK. (D). Cells were prepared as in (A) but treated with PQ-401 (10uM) 90 min prior to stimulation with IGF1. All results are representative of at least three independent experiments. Significant ($p<0.05$) *

when compared to non-treated group, # when compared to corresponding treated mimic control group.

Figure 6: Effect of miR378 on cell survival. (A) Immunofluorescence images of cardiomyocytes 72 h after either mock transfection (control), mimic control or 378-mimic, and following 4 h treatment with H2O2 (500 uM) showing To-Pro stained nuclei (blue), after TUNEL staining (green) and two images merged together. Arrows mark nuclei considered as TUNEL positive. (B) Quantification of TUNEL positive nuclei as per methods in different treatment groups. (C) Caspase 3/7 activity in cardiomyocytes transfected as in (A) and treated with H2O2 as indicated. # significantly different from non-treated group, * significant when compared to mock or mimic control transfected group treated with H2O2 for the same period (D) Western analysis of IGF1R and signaling cascade in cardiomyocytes transfected as in A and after 4 h of H2O2 treatment (E) Quantification of signal intensity of D. Expression levels of IGF1R, pIGF1R, Bim, Trail and Fas L were normalized with β-actin while that of pAkt, and pFoxO3 was normalized with their non-phospho counterparts. *$p<0.05$. Each bar is a mean ± SD of a minimum of 3 independent experiments.

Figure 7: miR-378 knockdown enhances IG1R expression and IGF1-induced AKT activation. (A) Northern showing knock-down of miR-378 in cardiac myocytes 48 h after transfection with either scramble control or 378-antimiR, U6 represent loading control on the same membrane. (B) Western analysis of IGF1R 72 h after transfection of cardiomyocytes with scramble or increasing amounts of 378-antimiR (C) Expression of pAkt and total Akt in cardiomyocytes transfected with scramble control or 378-antimiR. After 48 h of transfection, cells were incubated in serum free media overnight and then treated with IGF1 for 15 min. (D). Cells were prepared as in C and treated with IGF1R inhibitor PQ-401 (10 uM) 90 min prior to IGF1 treatment. Significant $p<0.05$ when *compared to non-PQ treated scramble control, # when compared to PQ-401 treated scramble control (n = 2).

Figure 8: miR-378 knockdown prevents H2O2 induced apoptosis program and hypoxia-reoxygenation induced cell death in an IGF1R-dependent manner. (A) Western analysis (duplicates) of p-IGF1R, IGF1R, and down-stream signaling cascade in response to oxidative stress following transfection with either scramble control or 378-antimiR. Same membrane was used again and again for probing with different antibodies after stripping (B) Quantification of signal intensity of A normalized essentially as described for 6E. (C) Time-course response of TUNEL positive nuclei in response to varying periods of hypoxia-re-oxygenation in presence of either scramble control or 378-antimiR (50 nM). Each bar is a mean ± SD of a minimum of 3 independent experiments. (D) Quantification of TUNEL positive nuclei as per methods in indicated treatment groups after 2 h of hypoxia followed by 2 h of re-oxygenation injury to cardiac myocytes. IGF1R inhibitor, PQ-401(PQ), produced a dose dependent inhibition of protective effects of 378-antimiR. (E) 378-antimiR enhanced cardiomyocytes viability. Significant ($p<0.05$) * when compared to scramble control group, # when compared to scramble PQ treated group.

Figure 9: miR-378 inhibition interferes with FOXO3 translocation in the cardiomyocyte nuclei. IGF1 is a negative regulator of miR378 (A) Confocal imaging showing FoxO3 subcellular distribution in co-cultures of neonatal cardiomyocyte and non-muscle cells 72 h after transfection with scramble control or 378-antimiR with and without H2O2 treatment for 4 hr. FoxO3 can be visualized as green immunofluorescence, nuclei as blue, myocytes as red immunofluorescence α-actinin positive cells and non-muscle cells as absence of red fluorescence. Note, with 378-antimiR transfection and H2O2 treatment FoxO3 was excluded only from the nuclei (seen as purple stained nuclei in the merged image) of red stained muscle

cells whereas its presence was detected in the nuclei of scramble control transfected muscle cells (seen as intense yellow staining in the merged image). (B) IGF1 expression and time course by Western in fetal and postnatal heart tissues and in cultured neonatal cardiac fibroblast (C) miR-378 overexpression does not significantly affect IGF1 expression in cardiomyocytes. (D) IGF1 acts as a negative regulator of miR-378. Primary cultures of cardiomyocytes were treated with increasing doses of IGF1 for 72 h. miR-378 expression analyzed by Northern. A modest but significant reduction was noted with higher dose of IGF1 (n=2).

FIGURE 1

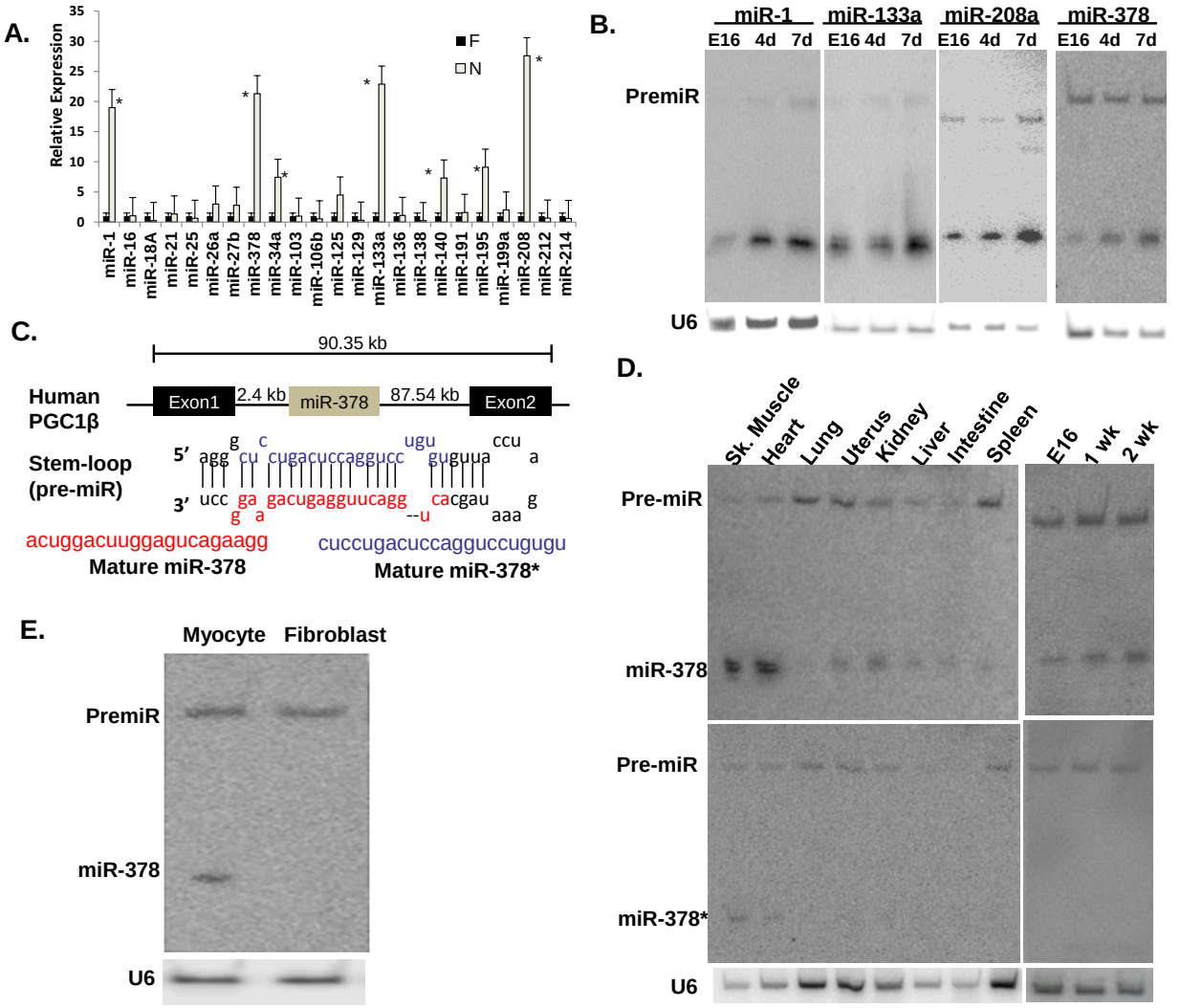
A.
Relative Expression
F
N
miR-1
miR-16
miR-18A
miR-21
miR-25
miR-26a
miR-27b
miR-378
miR-34a
miR-103
miR-106b
miR-125
miR-129
miR-133a
miR-136
miR-138
miR-140
miR-191
miR-195
miR-199a
miR-208
miR-212
miR-214
B.
miR-1
miR-133a
miR-208a
miR-378
E16 4d 7d
PremiR
U6
C.
90.35 kb
Human PGC1β
Exon1
2.4 kb
miR-378
87.54 kb
Exon2
Stem-loop (pre-miR)
acuggacuuggagucagaagg
Mature miR-378
cuccugacuccagguccugugu
Mature miR-378*
D.
Sk. Muscle
Heart
Lung
Uterus
Kidney
Liver
Intestine
Spleen
E16
1 wk
2 wk
Pre-miR
miR-378
Pre-miR
miR-378*
U6
E.
Myocyte
Fibroblast
PremiR
miR-378
U6

FIGURE 2

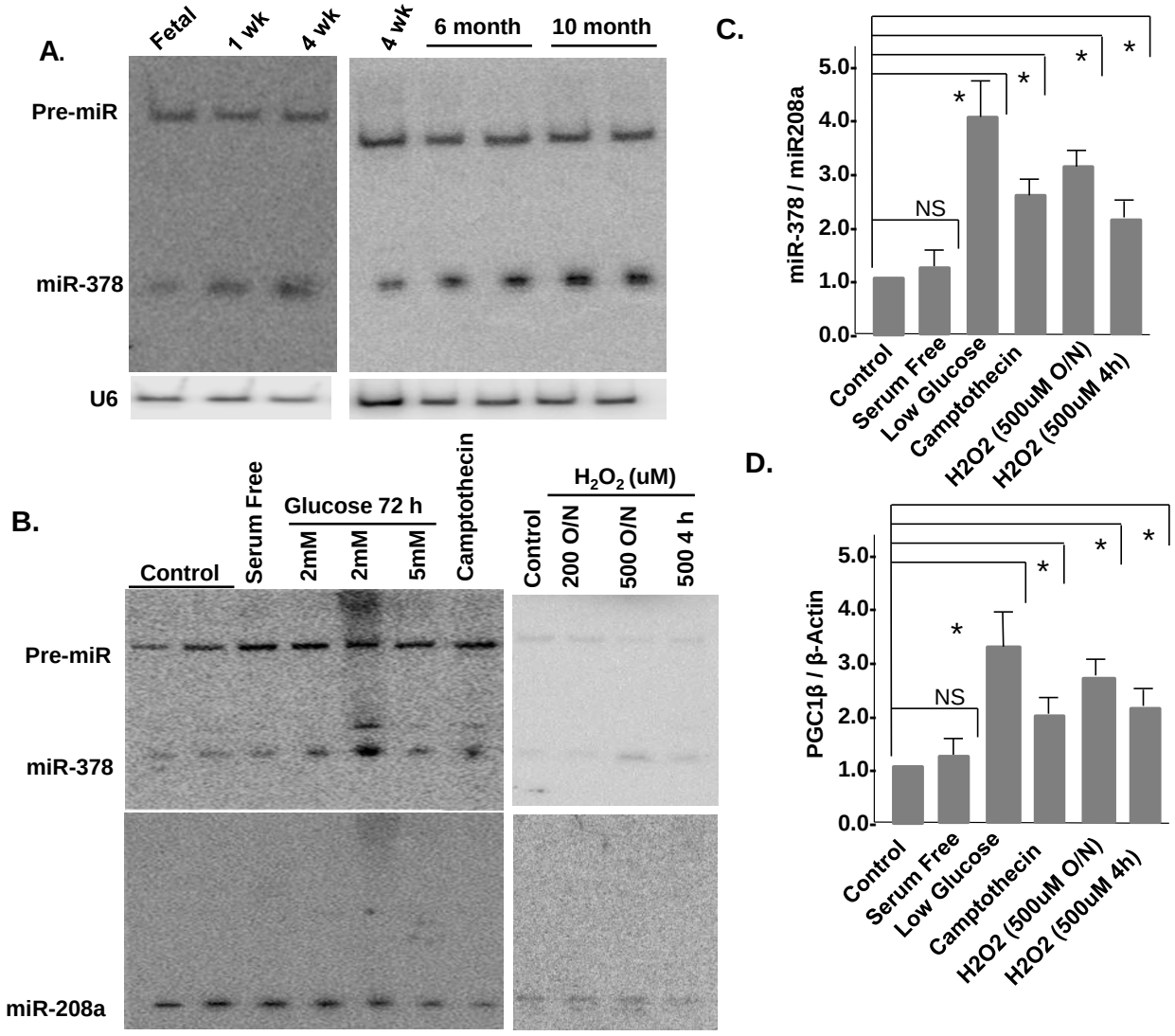
A.
Fetal
1 wk
4 wk
4 wk
6 month
10 month
Pre-miR
miR-378
U6
B.
Control
Serum Free
Glucose 72 h
2mM
2mM
5mM
Camptothecin
H2O2 (uM)
Control
200 O/N
500 O/N
500 4 h
Pre-miR
miR-378
miR-208a
C.
miR-378 / miR208a
NS
Control
Serum Free
Low Glucose
Camptothecin
H2O2 (500uM O/N)
H2O2 (500uM 4h)
D.
PGC1β / β-Actin
NS
Control
Serum Free
Low Glucose
Camptothecin
H2O2 (500uM O/N)
H2O2 (500uM 4h)

FIGURE 3

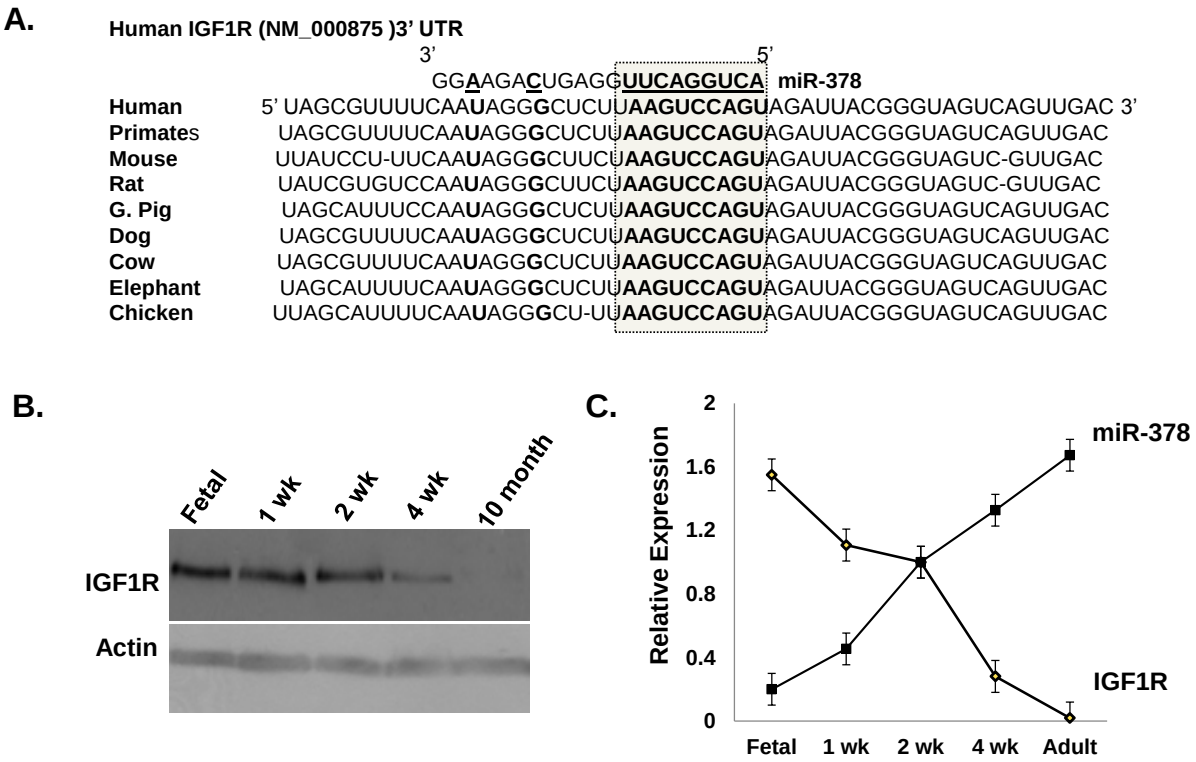
A.
Human IGF1R (NM_000875)3' UTR
3'
5'
GGAAGACUGAGGUUCAGGUCA miR-378
Human 5' UAGCGUUUUCAAUAGGGCUCUUAAGUCCAGUAGAUUACGGGUAGUCAGUUGAC 3'
Primates UAGCGUUUUCAAUAGGGCUCUUAAGUCCAGUAGAUUACGGGUAGUCAGUUGAC
Mouse UUAUCCU-UUCAAUAGGGCUUCUAAGUCCAGUAGAUUACGGGUAGUC-GUUGAC
Rat UAUCGUGUCCAAUAGGGCUUCUAAGUCCAGUAGAUUACGGGUAGUC-GUUGAC
G. Pig UAGCAUUUCCAAUAGGGCUCUUAAGUCCAGUAGAUUACGGGUAGUCAGUUGAC
Dog UAGCGUUUUCAAUAGGGCUCUUAAGUCCAGUAGAUUACGGGUAGUCAGUUGAC
Cow UAGCGUUUUCAAUAGGGCUCUUAAGUCCAGUAGAUUACGGGUAGUCAGUUGAC
Elephant UAGCAUUUUCAAUAGGGCUCUUAAGUCCAGUAGAUUACGGGUAGUCAGUUGAC
Chicken UUAGCAUUUUCAAUAGGGCU-UUAAGUCCAGUAGAUUACGGGUAGUCAGUUGAC
B.
Fetal
1 wk
2 wk
4 wk
10 month
IGF1R
Actin
C.
Relative Expression
2
1.6
1.2
0.8
0.4
0
miR-378
IGF1R
Fetal
1 wk
2 wk
4 wk
Adult

FIGURE 4

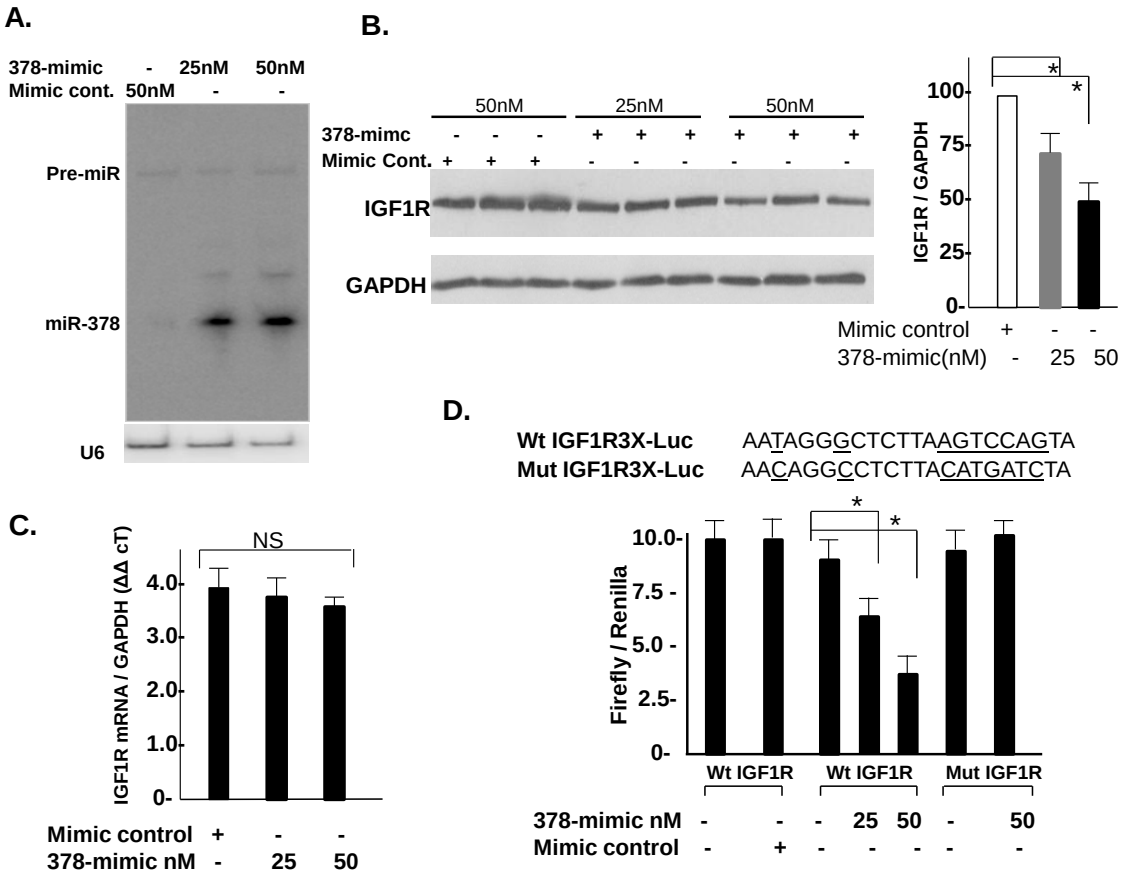
A.
378-mimic - 25nM 50nM
Mimic cont. 50nM - -
Pre-miR
miR-378
U6
B.
50nM 25nM 50nM
378-mimc - - - + + + + + +
Mimic Cont. + + + - - - - - -
IGF1R
GAPDH
IGF1R / GAPDH
100
75
50
25
0
*
*
Mimic control + - -
378-mimic(nM) - 25 50
C.
IGF1R mRNA / GAPDH (ΔΔ cT)
NS
4.0
3.0
2.0
1.0
0
Mimic control + - -
378-mimic nM - 25 50
D.
Wt IGF1R3X-Luc AATAGGGCTCTTAAGTCCAGTA
Mut IGF1R3X-Luc AACAGGCCTCTTACATGATCTA
Firefly / Renilla
10.0
7.5
5.0
2.5
0
*
*
Wt IGF1R
Wt IGF1R
Mut IGF1R
378-mimic nM - - - 25 50 - 50
Mimic control - + - - - - -

FIGURE 5

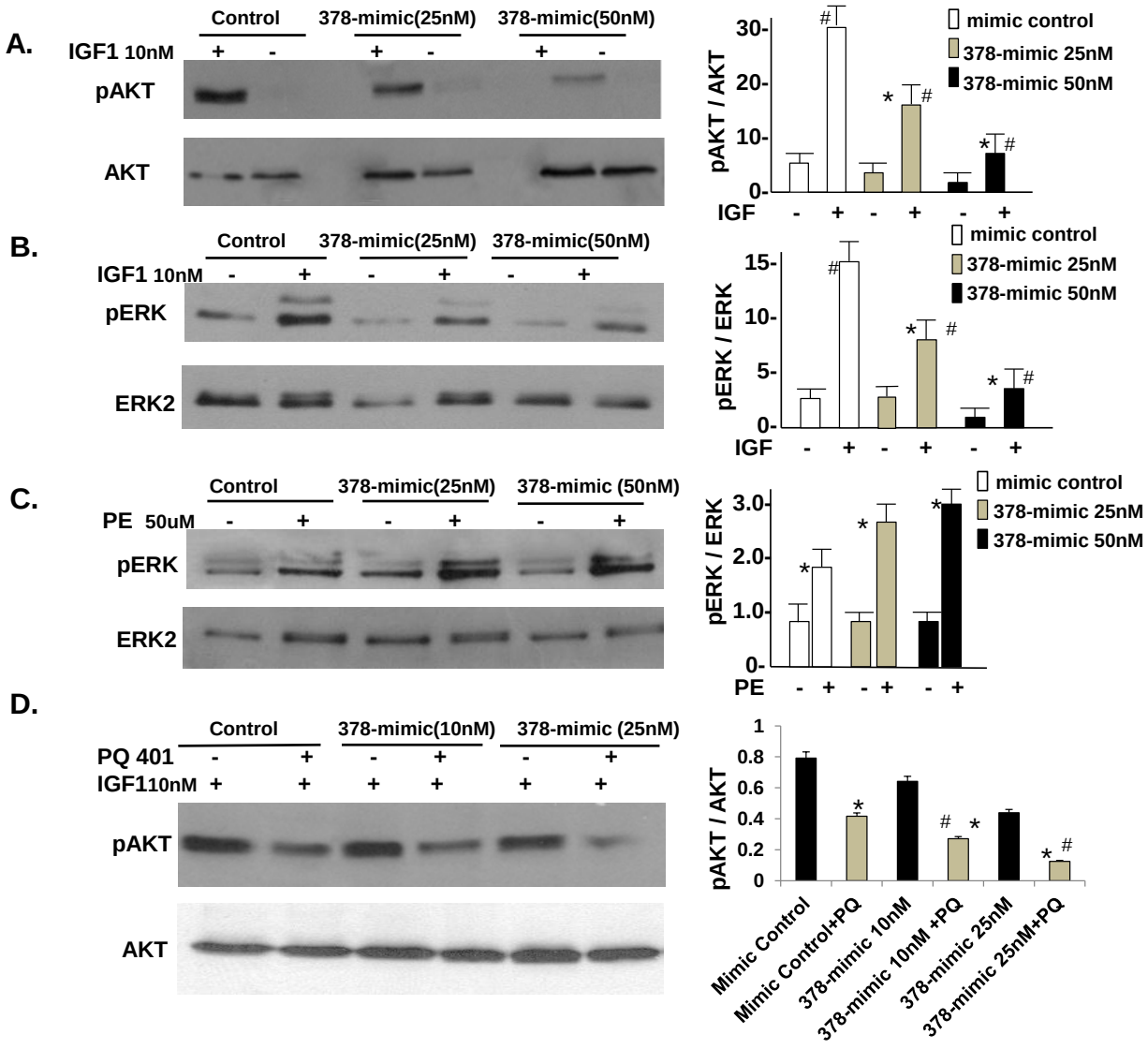
A.
Control
378-mimic(25nM)
378-mimic(50nM)
IGF1 10nM
pAKT
AKT
mimic control
378-mimic 25nM
378-mimic 50nM
pAKT / AKT
IGF
B.
pERK
ERK2
pERK / ERK
C.
PE 50uM
378-mimic (50nM)
D.
PQ 401
IGF1 10nM
378-mimic(10nM)
378-mimic (25nM)
Mimic Control
Mimic Control+PQ
378-mimic 10nM
378-mimic 10nM +PQ
378-mimic 25nM
378-mimic 25nM+PQ

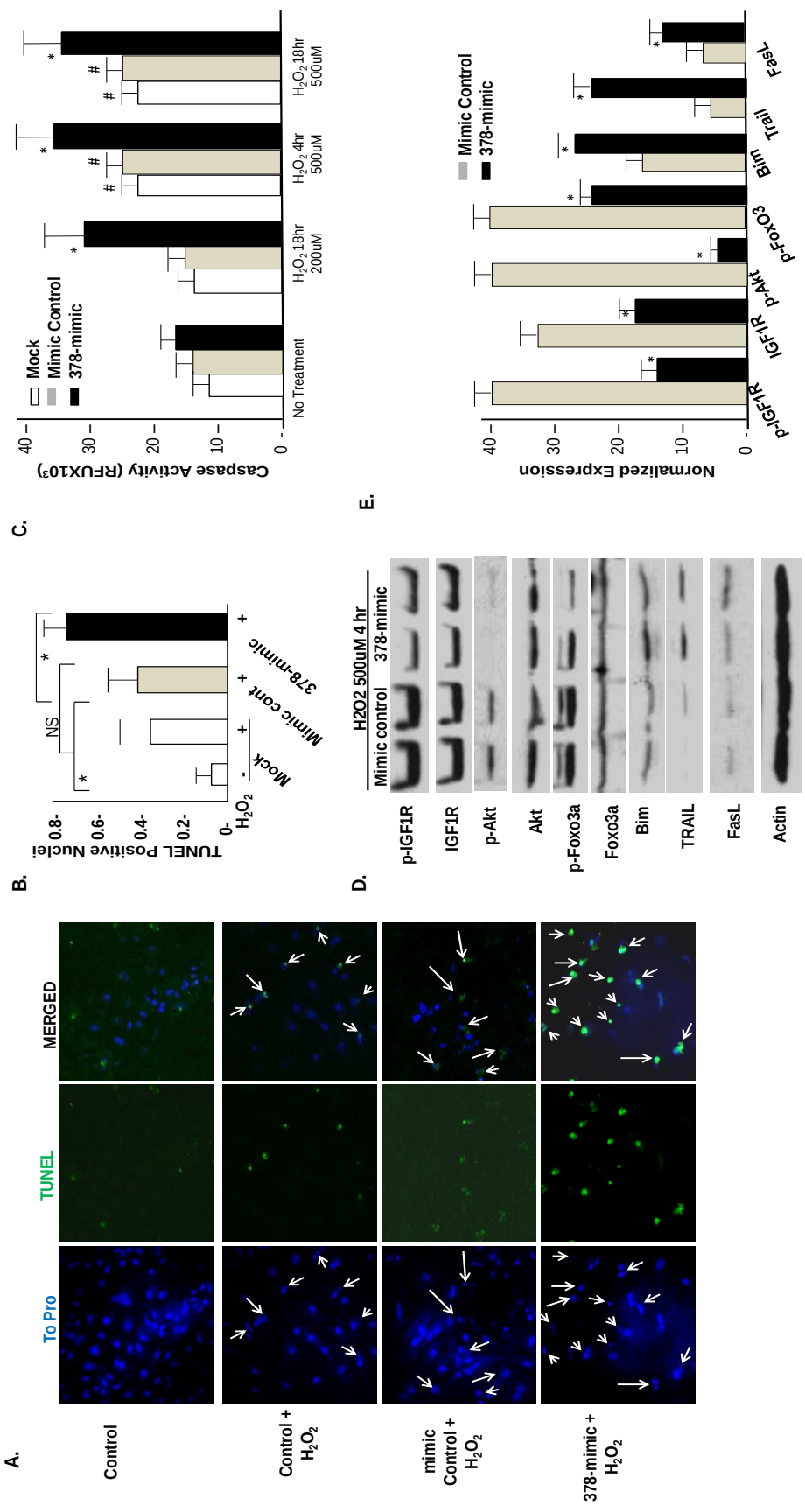
A.
Control
Control + H_2O_2
mimic Control + H_2O_2
378-mimic + H_2O_2
To Pro
TUNEL
MERGED
B.
TUNEL Positive Nuclei
0.8-
0.6-
0.4-
0.2-
0-
H_2O_2
Mock
Mimic cont
378-mimic
NS
C.
Caspase Activity (RFUX10³)
Mock
Mimic Control
378-mimic
No Treatment
H_2O_2 18hr 200uM
H_2O_2 4hr 500uM
H_2O_2 18hr 500uM
D.
H2O2 500uM 4 hr
Mimic control
378-mimic
p-IGF1R
IGF1R
p-Akt
Akt
p-Foxo3a
Foxo3a
Bim
TRAIL
FasL
Actin
E.
Normalized Expression
Mimic Control
378-mimic
p-IGF1R
IGF1R
p-Akt
p-Foxo3a
Bim
TrailI
FasL

FIGURE 6

FIGURE 7

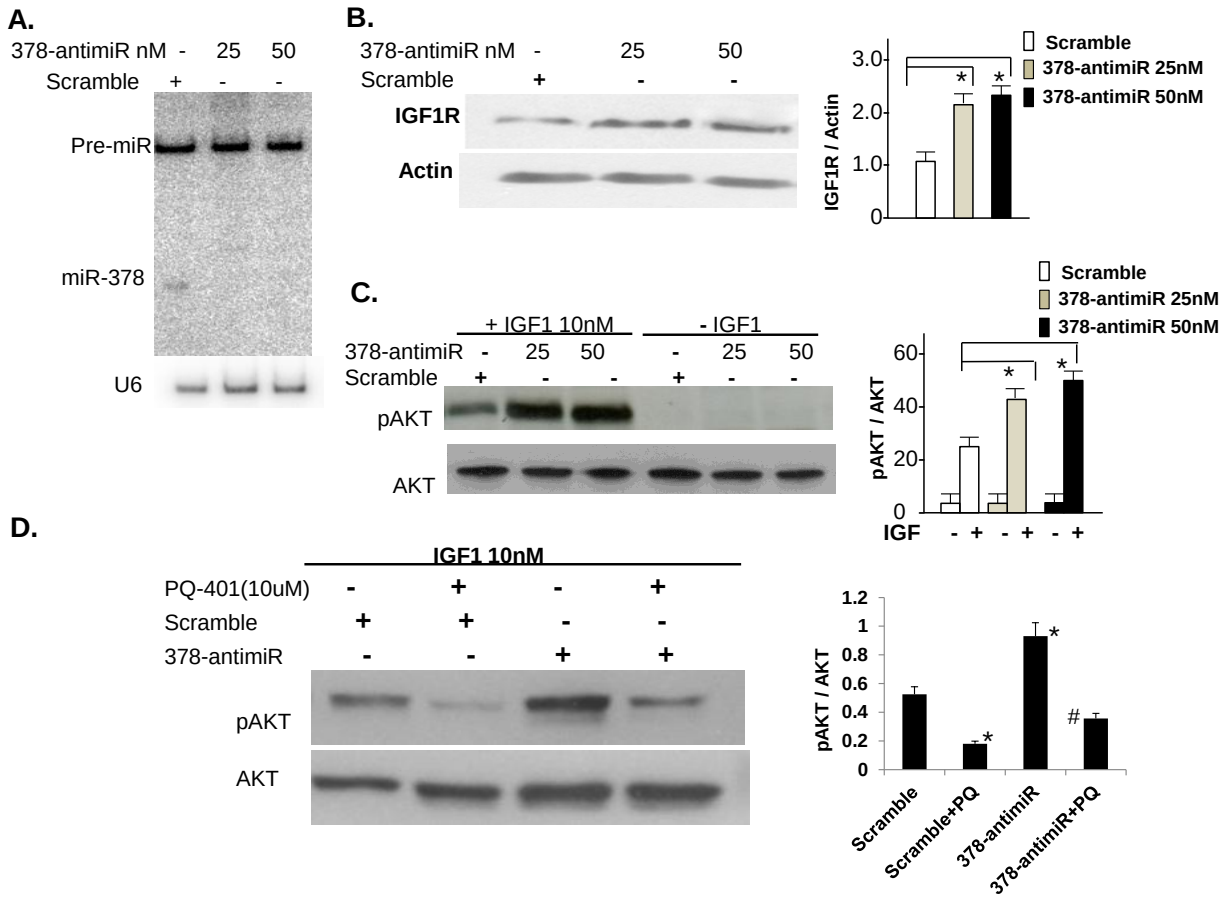
A.
378-antimiR nM - 25 50
Scramble + - -
Pre-miR
miR-378
U6
B.
378-antimiR nM - 25 50
Scramble + - -
IGF1R
Actin
IGF1R / Actin
Scramble
378-antimiR 25nM
378-antimiR 50nM
C.
+ IGF1 10nM
- IGF1
378-antimiR - 25 50 - 25 50
Scramble + - - + - -
pAKT
AKT
pAKT / AKT
IGF - + - + - +
D.
IGF1 10nM
PQ-401(10uM) - + - +
Scramble + + - -
378-antimiR - - + +
pAKT
AKT
pAKT / AKT
Scramble
Scramble+PQ
378-antimiR
378-antimiR+PQ

FIGURE 8

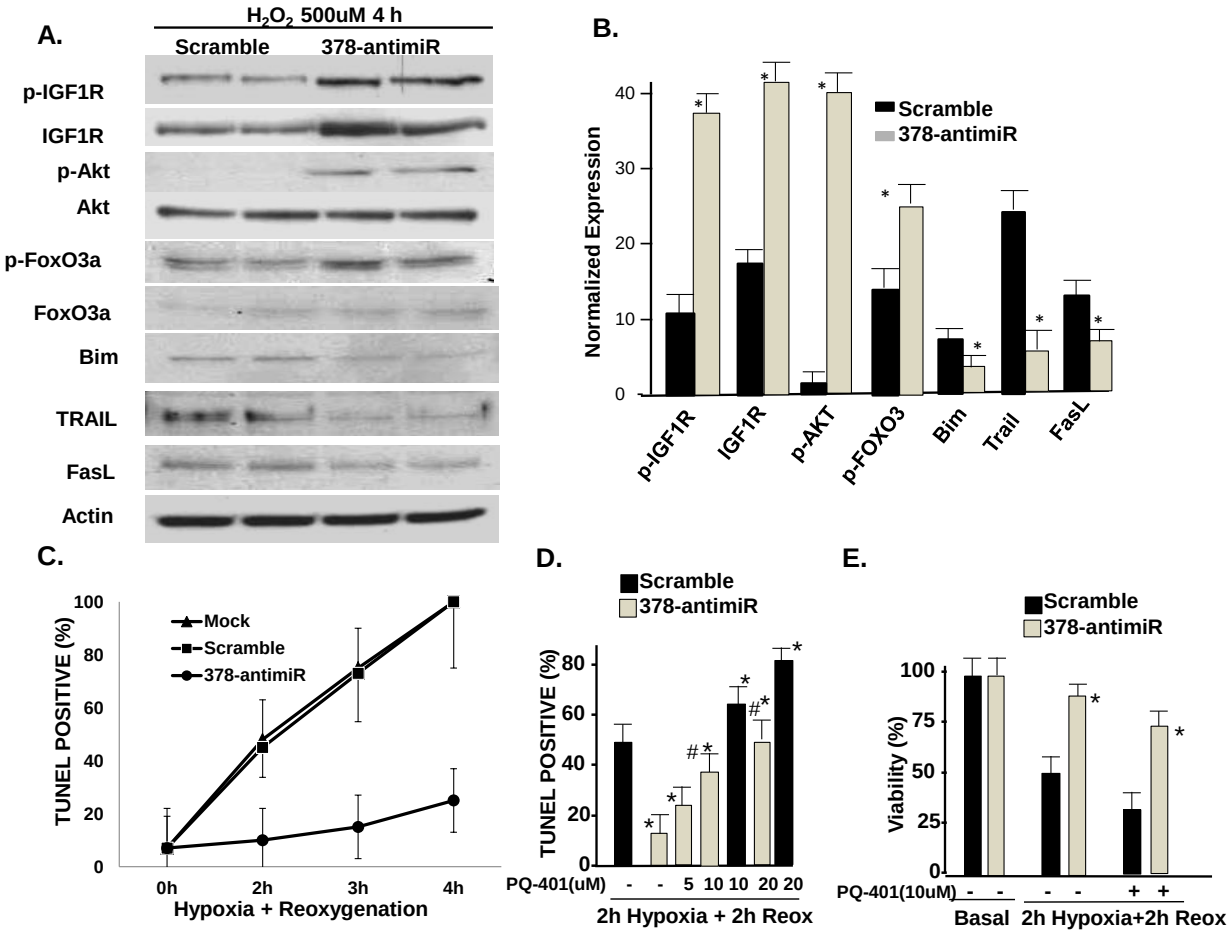
A.
H_2O_2 500uM 4 h
Scramble
378-antimiR
p-IGF1R
IGF1R
p-Akt
Akt
p-FoxO3a
FoxO3a
Bim
TRAIL
FasL
Actin
B.
Normalized Expression
Scramble
378-antimiR
p-IGF1R
IGF1R
p-AKT
p-FOXO3
Bim
Trail
FasL
C.
TUNEL POSITIVE (%)
Mock
Scramble
378-antimiR
Hypoxia + Reoxygenation
D.
Scramble
378-antimiR
TUNEL POSITIVE (%)
PQ-401(uM)
2h Hypoxia + 2h Reox
E.
Scramble
378-antimiR
Viability (%)
PQ-401(10uM)
Basal
2h Hypoxia+2h Reox

FIGURE 9

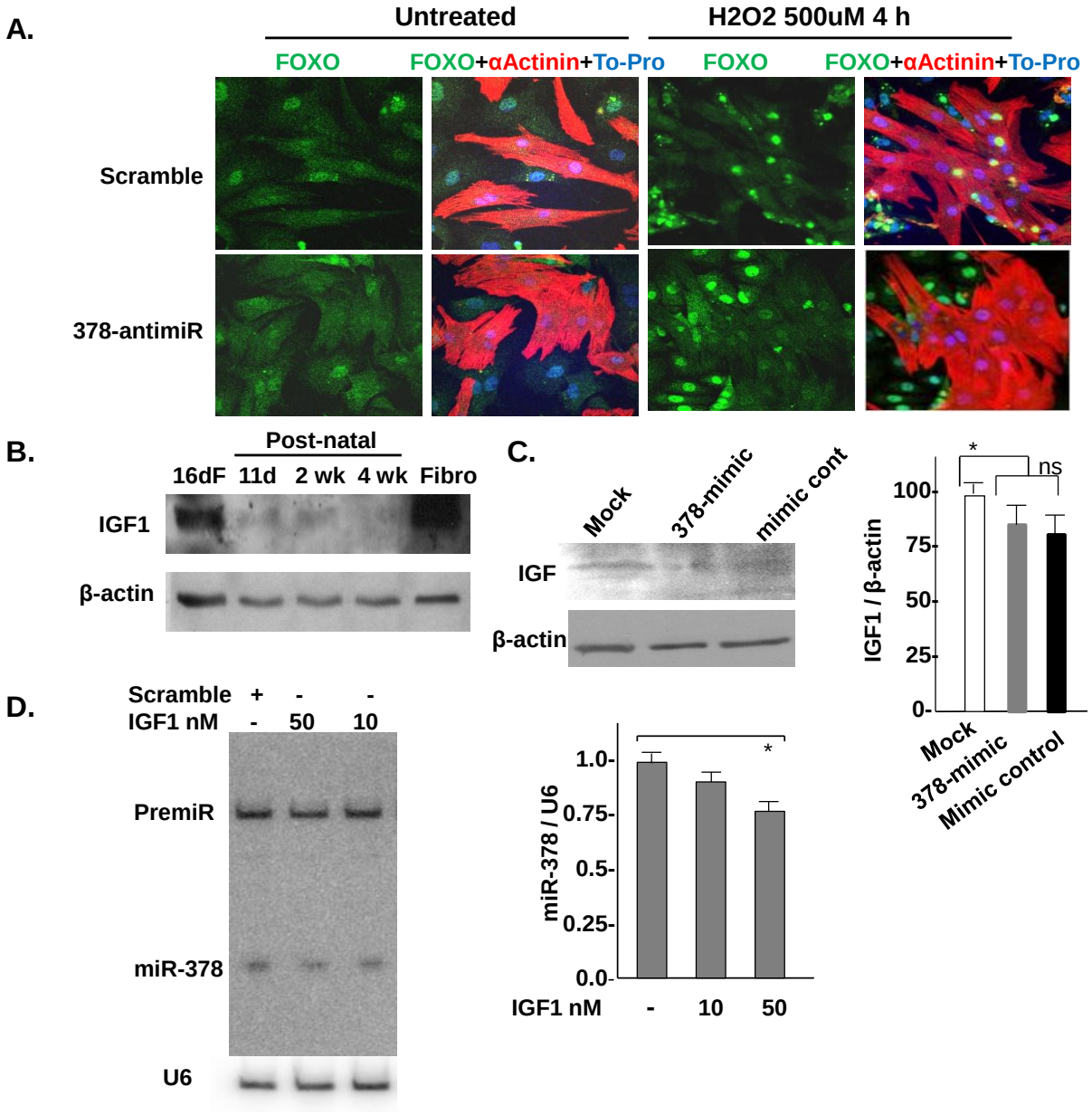
A.
Untreated
H2O2 500uM 4 h
FOXO
FOXO+αActinin+To-Pro
FOXO
FOXO+αActinin+To-Pro
Scramble
378-antimiR
B.
Post-natal
16dF 11d 2 wk 4 wk Fibro
IGF1
β-actin
C.
Mock
378-mimic
mimic cont
IGF
β-actin
IGF1 / β-actin
100
75
50
25
0
*
ns
Mock
378-mimic
Mimic control
D.
Scramble + - -
IGF1 nM - 50 10
PremiR
miR-378
U6
miR-378 / U6
1.0
0.75
0.5
0.25
0.0
*
IGF1 nM - 10 50